2024 European Control Conference (ECC)
June 25-28, 2024. Stockholm, Sweden

Observability Analysis of PEM Fuel Cell Systems with Anode Recirculation

Michael Hauck, Felix Petzke, Rania Tafat, Stefan Streif

Abstract— **The optimal control of gas partial pressures in fuel cell systems is a key part to increase the efficiency and the lifetime of the fuel cell. In automotive applications, the nitrogen and hydrogen gas partial pressures are not measurable with actual sensors. Therefore an observer is required to determine the gas partial pressures in the fuel cell system.**

In this paper we present an observability analysis for PEM fuel cell systems with anode recirculation for an automotive application. The fuel cell stack voltage and the total gas pressure in front of the fuel cell are assumed as measurable outputs. The opening of the input valve and purge valve as well as the total pressure at the cathode are inputs. The fuel cell stack current is a measurable disturbance. It is shown that the hydrogen and nitrogen partial pressures in front of the fuel cell, inside the fuel cell, and behind the fuel cell are globally differentially observable as long as the fuel cell system is not in idle mode. As a result, asymptotic and finite time observers can be used to observe the total pressures and partial hydrogen pressures in an fuel cell system with anode recirculation.

I. Introduction

The total pressure and gas partial pressures inside a fuel cell system and especially inside the fuel cell stack are key parameters for the optimal operation and avoiding of degradation of Proton Exchange Membrane (PEM) fuel cell systems [3], [15]. The higher the hydrogen partial pressure inside the fuel cell stack is, the higher is the fuel cell voltage, increasing the stack performance [17]. However, with an increase of the hydrogen partial pressure, the total pressure at the anode side increases, too. In order to avoid mechanical stress of the membrane, the cathode pressure is kept close to the anode pressure. This is usually done by an air compressor, consuming more energy, the higher the pressure is. Consequently, a high hydrogen partial pressure increases the performance of the fuel cell stack, but decreases the performance of the peripheral components and thereby possibly the overall system efficiency. Additionally, the optimal hydrogen partial pressure – balancing the performance of the stack and the components – depends on the requested fuel cell current. Furthermore, a minimum amount of hydrogen is required inside the fuel cell to avoid the phenomenon of fuel starvation, e.g. if the amount of available hydrogen in a fuel cell is not large enough, the fuel cell electrodes starts to degrade, resulting in a reduced fuel cell lifetime and performance [7], [18]. Therefore, a controller is required to track the optimal hydrogen partial pressure.

The authors are with Technische Universität Chemnitz, 09126 Chemnitz, Germany, Automatic Control and System Dynamics Lab (e-mail: {michael.hauck, felix.petzke, rania.tafat, stefan.streif}@etit.tu-chemnitz.de)

This research has been performed as part of the project ReSIDA-H2. This project was funded by the European Social Fund Plus (ESF Plus) and the Free State of Saxony.

Additionally, the nitrogen partial pressure in the fuel cell systems needs to be controlled. Resulting from the nitrogen partial pressure difference between the air in the cathode side and the hydrogen containing gas mixture at the anode side, nitrogen permeates from the cathode to the anode and accumulates there due to the recirculation of the anode gas mixture [2]. To avoid large nitrogen partial pressures in the anode, a purge valve is used to remove impurities from the anode regularly. In the literature, a maximum tolerable nitrogen partial pressure of 3-5% was identified [20], [23]. Hence, not only the partial pressure of hydrogen but also the one of nitrogen needs to be determined to control its value. However, it is generally very challenging or outright infeasible to implement partial gas pressure sensors inside the fuel cell stack [15]. Furthermore, current gas partial pressure sensors are expensive, suffer from slow response times, low accuracy, and would significantly increase the total system costs [3]. To tackle these challenges, it is desirable to estimate the pressure inside the anode and the gas partial pressures in different control volumes of the anode recirculation system from already available measurements. The goal of this work is to prove observability of these internal states using only the stack voltage and total pressure at the anode inlet as measurable values.

In the existing literature, different mathematical models of fuel cell systems are investigated with respect to their observability, which differ in their assumptions, depth of detail, choice of state variables, and measurable outputs. The observability of a linear fuel cell model without anode recirculation and nitrogen permeation was analyzed in [19], under the assumptions, that the cathode is fully humidified and no liquid condensation occurs. By measuring the compressor air flow rate, supply manifold pressure, and fuel cell stack voltage, observability of the hydrogen partial pressure at the anode, gas partial pressures at the cathode, and total pressures in cathode flow system was shown.

A linearized 24-state model of the water distribution in a fuel cell system was used in [16] to show observability of cathode gas concentrations, concentration of hydrogen at the anode, and water distribution at the anode by measuring the stack voltage and the relative humidity in the fuel cell channels. The observability of another linearized high-order fuel cell system model, containing also a model of the hydrogen reforming process, was shown in [12].

In [21], the observability of a linearized fuel cell pressure model was shown, by measuring the anode hydrogen pressure and the cathode oxygen pressure. However, measuring the gas partial pressures in the fuel cell stack is a challenging

task in practical applications. That is why this measurements should be avoided by designing an observer.

In all these observability analyses, linearized fuel cell models without anode recirculation and nitrogen permeation from the cathode to the anode are used. There exist only few observability analysis for nonlinear fuel cell models.

In [14], the observability of gas concentrations in a fuel cell system without recirculation was analyzed. Therein, the gas concentrations at the outlet of the cathode and anode were assumed as measurable inputs. Then a nonlinear distributed parameter observer was presented to observe the hydrogen and water partial pressures at the anode and all gas partial pressures at the cathode. The observer is based on measuring the hydrogen and water partial pressures at the outlet of the anode and all gas partial pressures at the outlet of the cathode. During the simulations, the rank of the Jacobian of the observability map was calculated numerically depending on the current states. The observer was disconnected as long as the rank was lower than the expected full rank. The same approach was used in [15], but with different inputs variables, which influences the observability due to the non-linearity of the system. Here, only the inlet gas flows are used as input variables in contrast to [14], where in addition also the internal water and reaction flows are used as inputs. In both approaches, the hydrogen pressure is calculated directly by the difference of total pressure and water partial pressure. However, in the presence of accumulating nitrogen, this approach is not valid.

In addition to these observability analyses, there exists some literature for observer design in fuel cell systems without analyzing the observability. There are different approaches for estimating total or partial gas pressures in fuel cell systems using nonlinear observer approaches. In [3], a nonlinear observer of the inlet and outlet hydrogen partial pressures was developed under the assumptions, that the hydrogen partial pressure changes slowly and that the total pressures at the inlet, inside, and at the outlet of the anode are known.

An unscented Kalman filter was used in [22] with an adaption of the process noise covariance matrix to estimate the water and hydrogen mass in the fuel cell. Therefore, the some internal states like water mass in anode and cathode and temperature are assumed to reached their steady-state values.

The existing approaches use simplified models, e.g. linearized models or simplified setups without anode recirculation, without nitrogen accumulation or unrealistic assumptions for automotive setups like slow pressure changes or measurability of gas partial pressures.

This paper analyzes, under which conditions it is possible to estimate the total pressures and gas partial pressures in different control volumes of a nonlinear fuel cell model with anode recirculation. It is assumed, that the total pressure in front of the fuel cell stack and the stack voltage are measured. These are all standard sensors in automotive applications. In Section II, the model is presented. Afterwards, global differential observability is shown for this setup and local differential observability under the assumption that only the stack voltage is measurable.

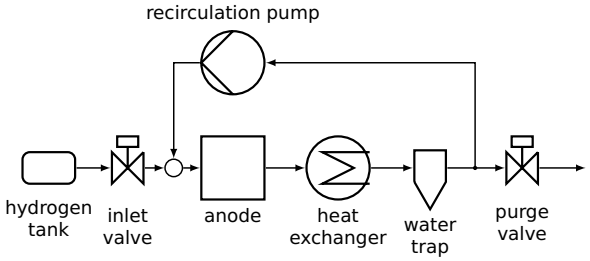

Fig. 1: Principle sketch of an anode recirculation system [10]

II. PROBLEM SETTING

In this section, the model of a PEM fuel cell system with anode recirculation is developed. Fig. 1 shows the basic components of the anode recirculation system. Hydrogen is stored under high pressure in the hydrogen tank. The inlet valve controls the amount of incoming hydrogen. Inside the anode, the hydrogen molecules are split and permeate through a membrane into the cathode, where they react with oxygen to produce water. In addition, gaseous impurities – especially nitrogen – permeate from the cathode through the membrane into the anode. These gaseous impurities and unconsumed hydrogen are recirculated by a recirculation pump. To avoid a large accumulation of the nitrogen, the purge valve is opened regularly to remove the impurities [9]. In [10], a control-oriented model of a PEM fuel cell systems with anode recirculation was modeled. Therein, the anode recirculation system is divided into three control volumes V_i: V_1 contains the pipe work and the equipment for measurement in front of the fuel cell stack, V_2 is the volume of the actual anode within the fuel cell stack, and V_3 contains the heat exchanger, the water trap the pipe work, as well as the equipment for measurement behind the fuel cell stack.

Let the state vector be defined via the total pressures and hydrogen partial pressures in the control volumes as

$$x = \left(p_1, p_2, p_3, p_{\mathrm{H}_2,1}, p_{\mathrm{H}_2,2}, p_{\mathrm{H}_2,3}\right)^\top,$$

where p_i is the total pressure and $p_{\mathrm{H}_2,i}$ the partial hydrogen pressure in the volume V_i. Under the assumption, that the gases in the different control volumes are at 100% relative humidity, the nitrogen partial pressures can be calculated by the difference of the total pressure and the hydrogen and water partial pressure. The inputs and the measurable disturbance are summarized as vector

$$u = [u_\mathrm{in}, u_\mathrm{purge}, p_\mathrm{ca}, i_\mathrm{fc}],$$

where u_in is the opening of the input valve, u_purge the opening of the purge valve, p_ca the pressure at the cathode side of the fuel cell and i_fc the fuel cell stack current.

The total pressure in the control volumes is modeled via a balance equation of the gas flows [13]

$$\dot{p}_i = \frac{R_i T_i}{V_i} \sum_j W_j$$

with R_i is the gas constant and T_i the temperature of the gas mixture in control volume V_i. The gas flows between the control volumes are modeled based on a pressure difference [9]

$$W_{i,j} = k_{i,j}\sqrt{p_i - p_j}$$

with the flow constant $k_{i,j}$. Similarly, the incoming gas flow through the input valve is given by

$$W_{\text{in}} = k_{\text{in}}\sqrt{p_{\text{tank}} - p_1}u_{\text{in}}$$

and the purged gas flow through the purge valve as

$$W_{\text{purge}} = k_{\text{purge}}\sqrt{p_3 - p_0}u_{\text{purge}},$$

where p_{tank} is the pressure after the hydrogen tank and p_0 the ambient pressure.

The hydrogen and nitrogen permeation through the membrane are modeled as

$$\begin{aligned} W_{\text{H}_2,\text{react}} &= k_{\text{H}_2} i_{\text{fc}}, \\ W_{\text{N}_2,\text{diff}} &= k_{\text{N}_2} p_{\text{N}_2,\text{ca}}, \end{aligned}$$

where k_{H_2} and k_{N_2} are permeation coefficients [4]. Similarly, the partial hydrogen pressures in the control volumes are calculated based on the partial hydrogen gas flows.

Transformed into state-space, the system dynamics are represented as follows:

$$\begin{aligned} \dot{x} =& f(x,u) \\ =& \begin{pmatrix} -a_1\sqrt{x_1 - x_2} \\ a_4\sqrt{x_1 - x_2} - a_6\sqrt{x_2 - x_3} \\ a_7\sqrt{x_2 - x_3} \\ -a_1\sqrt{x_1 - x_2}\dfrac{x_4}{x_1} \\ a_4\sqrt{x_1 - x_2}\dfrac{x_4}{x_1} - a_6\sqrt{x_2 - x_3}\dfrac{x_5}{x_2} \\ a_7\sqrt{x_2 - x_3}\dfrac{x_5}{x_2} \end{pmatrix} \\ &+ \begin{pmatrix} a_2\sqrt{p_{\text{tank}} - x_1} \\ 0 \\ 0 \\ a_2\sqrt{p_{\text{tank}} - x_1} \\ 0 \\ 0 \end{pmatrix} u_{in} + \begin{pmatrix} 0 \\ a_5 \\ 0 \\ 0 \\ 0 \\ 0 \end{pmatrix} p_{ca} \\ &+ \begin{pmatrix} 0 \\ 0 \\ -a_9\sqrt{x_3 - p_0} \\ 0 \\ 0 \\ -a_9\sqrt{x_3 - p_0}\dfrac{x_6}{x_3} \end{pmatrix} u_{purge} + \begin{pmatrix} a_3 \\ -a_{11} \\ -a_8 \\ a_3\dfrac{x_6}{x_3} \\ -a_{11} \\ -a_8\dfrac{x_6}{x_3} \end{pmatrix} i_{\text{fc}}, \end{aligned} \tag{1}$$

where a_i are aggregated positive constants.

In the literature, different physical values are assumed as measured outputs. In [3], the fuel cell stack voltage, oxygen partial pressure at the cathode and total pressures in front, inside and behind the anode, are assumed as measured outputs. Additionally, water partial pressures in the anode and cathode, as well as the temperature are measured in [22].

However, only the stack voltage and total pressures outside of the fuel cell are used in state of the art automotive fuel cell applications, since partial gas pressures are difficult and expensive to measure actually. To reduce the costs of the sensors, only the total pressure in front of the fuel cell p_1 and the stack voltage V_{fc} are assumed to be measured. Hence, the output is given by $y = (p_1, V_{\text{fc}})^T$.

The stack voltage is determined based on an automotive stack voltage model developed in [19] for a FORD P2000 fuel cell prototype vehicle [1]. Under the assumption of n_{cell} connected equal cells, the stack voltage is given by

$$U_{\text{stack}} = n_{\text{cell}} U_{\text{cell}}.$$

The single cell voltage U_{cell} is calculated based on the open circuit voltage U_{rev} and different kinds of voltage losses

$$U_{\text{cell}} = U_{\text{rev}} - U_{\text{act}} - U_{\text{ohm}} - U_{\text{conc}},$$

where U_{act} is the activation loss, U_{ohm} is the ohmic loss, and U_{conc} the concentration loss. They are given by

$$\begin{aligned} U_{\text{rev}} &= k_1 + k_2\left(\ln(p_{\text{H}_2}) + 0.5\ln(p_{\text{O}_2})\right), \\ U_{\text{act}} &= k_3 + k_4(1 - e^{-k_5 i_{\text{fc}}}), \\ U_{\text{ohm}} &= i_{\text{fc}} k_6, \\ U_{\text{conc}} &= i_{\text{fc}} k_7 i_{\text{fc}}^{k_8}, \end{aligned}$$

where p_{H_2} the partial hydrogen pressure in the anode, p_{O_2} the partial oxygen pressure in the cathode, and i_{fc} the requested cell current. The parameters k_{i} are listed in [19]. Therefore, the output function can be expressed by

$$y = h(x,u) = \begin{pmatrix} x_1 \\ a_{13}\ln(x_5) + h_u(u_4) \end{pmatrix} \tag{2}$$

with $h_u(u_4) = a_{12} + a_{14}e^{-a_{15}u_4} - a_{15}u_4 - a_{16}u_4^3$.

In the following, physically motivated boundaries on the states, inputs and outputs are noted.

Assumption 1: The total gas pressures are modeled as one-directional gas flows from the high pressure tank to the ambient pressure. Therefore, it holds that $p_{\text{tank}} > p_1 > p_2 > p_3 > p_0 > 0$. Note that this implies, that all the square roots in equation (1) and in further calculations have positive non-zero radicands and therefore nonzero real values. Additionally, dividing by $p_i - p_j$ is always possible. □

Assumption 2: In each control volume, the total pressure is larger than the hydrogen partial pressure, since the total pressure is the sum of the different gas partial pressures, i.e. $p_1 \geq p_4 > 0$, $p_2 \geq p_5 > 0$, and $p_3 \geq p_6 > 0$. □

Assumption 3: The inputs $u_i \geq 0$ are physically limited to positive values. Due to the mechanics of the valve openings, pressure build-up, and the chemistry inside the fuel cell, all inputs and outputs are analytic functions w.r.t. time. □

Remark 1: All parameters a_i are non-zero aggregated physical constants. □

In the next section, the observability of the presented model is analyzed.

III. Observability Analysis

For the remainder of this paper we use the following definition of global observability for nonlinear systems.

Definition 1 (Global Differential Observability [5], [6]): Consider the nonlinear system

$$\dot{x} = f(x,u), \quad y = h(x,u) \tag{3}$$

with $x \in \mathcal{X} \subset \mathbb{R}^{d_x}$ denoting the state, $u \in \mathcal{U} \subset \mathbb{R}^{d_u}$ the input, and $y \in \mathbb{R}^{d_y}$ the output, respectively. Let $u^{[m]} = \left(u(t), \dot{u}(t), \dots, u^{(m-1)}\right) \in \mathcal{U}^m$ denote the vector of the input and its derivatives. Furthermore, consider the function

$$\mathcal{H}(x,u^{[m]}) = \begin{pmatrix} h(x,u^{[m]}) \\ L_f h(x,u^{[m]}) \\ \vdots \\ L_f^{m-1} h(x,u^{[m]}) \end{pmatrix}.$$

System (3) is called globally differentially observable of order m on $\mathcal{X}$ if for any $x \in \mathcal{X}$ and $u^{[m]} \in \mathcal{U}^m$, the map $x \mapsto \mathcal{H}(x,u^{[m]})$ is injective on $\mathcal{X}$, with $L_f^m h(x,u^{[m]}) = \frac{d^m y}{dt^m}$ being the m-th order Lie-derivative of h. □

Note that for nonlinear systems, it is often hard to show, that the map $\mathcal{H}(x,u^{[m]})$ is injective *globally*. Therefore, often only local differential observability is analyzed by showing that the map $\mathcal{H}_m(x,u^{[m]})$ is injective in a neighborhood $\mathcal{X}_N \subset \mathbb{R}^{d_x}$ of $x^0 \in \mathcal{X}$. This is usually done by proving, that the Jacobian of $\mathcal{H}_m(x,u^{[m]})$ has full rank [11].

In the following it is shown, that System (1) is globally differentially observable of order 3, according to Definition 1. To this end, the map $\mathcal{H}(x,u^{[3]})$ is calculated explicitly and then shown to be globally injective. In a first step, the map

$$\mathcal{H}(x,u^{[3]}) = \begin{pmatrix} y_1 \\ y_2 \\ \dot{y}_1 \\ \dot{y}_2 \\ \ddot{y}_1 \\ \ddot{y}_2 \end{pmatrix} = \begin{pmatrix} h_1(x,u^{[3]}) \\ h_2(x,u^{[3]}) \\ L_f h_1(x,u^{[3]}) \\ L_f h_2(x,u^{[3]}) \\ L_f^2 h_1(x,u^{[3]}) \\ L_f^2 h_2(x,u^{[3]}) \end{pmatrix}$$

is proposed. If it is clear from the context, the general dependency on $(x,u^{[3]})$ is omitted for the sake of brevity. The first entries are the output functions

$$h_1 = x_1 \tag{4}$$

$$h_2 = a_{13}\ln(x_5) + h_u(u_4) \tag{5}$$

according to (2).

The first Lie-derivatives $L_f h_1$ and $L_f h_2$ of functions h_1 and h_2, respectively, are calculated as

$$\begin{aligned} L_f h_1 &= \frac{\partial h_1}{\partial x}\frac{\partial x}{\partial t} + \frac{\partial h_1}{\partial u}\frac{\partial u}{\partial t} = \dot{x}_1 \\ &= -a_1\sqrt{x_1 - x_2} + a_2\sqrt{p_{\text{tank}} - x_1}u_1 + a_3 u_4 \end{aligned} \tag{6}$$

$$\begin{aligned} L_f h_2 &= \frac{a_{13}}{x_5}\dot{x}_5 + \frac{\partial h_u(u_4)}{\partial u_4}\frac{\partial u_4}{\partial t} \\ &= \frac{a_{13}}{x_5}\left(a_4\sqrt{x_1 - x_2}\frac{x_4}{x_1} - a_6\sqrt{x_2 - x_3}\frac{x_5}{x_2} - a_{11}u_4\right) \\ &\quad + \frac{\partial h_u(u_4)}{\partial u_4}\frac{\partial u_4}{\partial t}, \end{aligned} \tag{7}$$

where $\frac{\partial h_u(u_4)}{\partial u_4}\frac{\partial u_4}{\partial t}$ only depends on constant parameters and the measurable input u_4 and its derivative $\dot{u}_4$. For ease of notation, this term is denoted as $\dot{h}_u(u_4)$.

Now, the second Lie-derivative $L_f^2 h_1$ is given by

$$L_f^2 h_1 = \frac{\partial L_f h_1}{\partial x}\frac{\partial x}{\partial t} + \frac{\partial L_f h_1}{\partial u}\frac{\partial u}{\partial t}, \tag{8}$$

with

$$\begin{aligned} \frac{\partial L_f h_1}{\partial x}\frac{\partial x}{\partial t} &= -\left(\frac{a_1}{2\sqrt{x_1 - x_2}} + \frac{a_2 u_1}{2\sqrt{p_{\text{tank}} - x_1}}\right) \\ &\quad \left(a_3 u_4 - a_1\sqrt{x_1 - x_2} + a_2 u_1\sqrt{p_{\text{tank}} - x_1}\right) \\ &\quad - \frac{a_1(a_{11}u_4 - a_5 u_3 - a_4\sqrt{x_1 - x_2})}{2\sqrt{x_1 - x_2}} \\ &\quad + \frac{a_6\sqrt{x_2 - x_3}}{2\sqrt{x_1 - x_2}} \\ &= \mathcal{O}_1(x_1,x_2,u) + \frac{a_6\sqrt{x_2 - x_3}}{2\sqrt{x_1 - x_2}} \end{aligned}$$

and

$$\frac{\partial L_f h_1}{\partial u}\frac{\partial u}{\partial t} = a_2\sqrt{p_{\text{tank}} - x_1}\dot{u}_1 + a_3\dot{u}_4.$$

Similarly, the second Lie-derivative $L_f^2 h_2$ is given by

$$L_f^2 h_2 = \frac{\partial L_f h_2}{\partial x}\frac{\partial x}{\partial t} + \frac{\partial L_f h_2}{\partial u}\frac{\partial u}{\partial t}, \tag{9}$$

with

$$\frac{\partial L_f h_2}{\partial x}\frac{\partial x}{\partial t} = \mathcal{O}_2(x_1,\dots,x_5,u)x_6 + \mathcal{O}_3(x_1,\dots,x_5,u)$$

and

$$\frac{\partial L_f h_2}{\partial u}\frac{\partial u}{\partial t} = \mathcal{O}_4(x_5,u,\dot{u},\ddot{u}).$$

For the sake of clarity, only the linear dependency on x_6 is explicitly presented here, since it is needed for further calculations. The full equations for $\mathcal{O}_i(\cdot)$ are listed in the appendix.

In the next step it is shown, that the presented map $\mathcal{H}$ is an injective globally on $\mathcal{X}$. This means, that the states x can be uniquely reconstructed by the measured outputs y and the known inputs u and their derivatives $\dot{y}$, $\ddot{y}$, $\dot{u}$ and $\ddot{u}$.

From Equation (4) we get

$$x_1 = y_1. \tag{10}$$

Equation (5) contains only one unknown state and can be rearranged as

$$x_5 = e^{\frac{y_2 - h_u(u_4)}{a_{13}}}. \tag{11}$$

So the state x_5 can be reconstructed by the measurable inputs and outputs.

According to Equation (6), $\dot{y}_1$ depends on the inputs and the states x_1 and x_2. Using Equation (10), it can be rewritten as

$$x_2 = y_1 - \left(\frac{\dot{y}_1 - a_2\sqrt{p_{\text{tank}} - y_1}u_1 - a_3 u_4}{a_1} \right)^2. \tag{12}$$

Hence, x_2 can be determined by the measurable variables for $a_1 \neq 0$.

By rearranging Equation (7), the state x_4 can be determined by

$$x_4 = \frac{x_1}{a_4\sqrt{x_1 - x_2}} \cdot \left((\dot{y}_2 - \dot{h}_u(u_4))\frac{x_5}{a_{13}} + a_6\sqrt{x_2 - x_3}\frac{x_5}{x_2} + a_{11}u_4 \right), \tag{13}$$

with x_1, x_2 and x_5 according to Equations (10) - (12) , $a_4, a_{13}, x_2 \neq 0$, and $x_1 > x_2$.

The state x_3 can be determined by rearranging Equation (8) as

$$x_3 = -\left(\ddot{y}_1 - \mathcal{O}_1(x_1, x_2, u) - a_2\sqrt{p_{\text{tank}} - x_1}\dot{u}_1 - a_3\dot{u}_4 \right)^2 \cdot \frac{4(x_1 - x_2)}{a_6^2} + x_2, \tag{14}$$

where the states x_1 and x_2 are given by Equations (10) and (12), respectively. Hence, x_3 can be reconstructed for $a_6 > 0$ and $p_{\text{tank}} > x_1 > x_2$.

The state x_6 is determined by rearranging Equation (9)

$$x_6 = \frac{\ddot{y}_2 - \mathcal{O}_3(x_1, \ldots, x_5, u) - \mathcal{O}_4(x_5, u, \dot{u}, \ddot{u})}{\mathcal{O}_2(x_1, \ldots, x_5, u)} \tag{15}$$

where the states $x_1, \ldots x_5$ are given by Equations (10) - (14). Therefore, the last state x_6 can be reconstructed for $x_1, x_2, x_5 > 0$, $p_{\text{tank}} > x_1 > x_2 > x_3 > p_0$ and $\mathcal{O}_2 \neq 0$ resulting in $a_3, a_4 a_{13} \neq 0$ and $u_4 \neq 0$.

IV. Discussion

As shown in the last chapter, $\mathcal{H}$ is injective under the following conditions:

- $a_1, a_3, a_4, a_6, a_{13} \neq 0$,
- $x_1, x_2, x_5 \neq 0$,
- $p_{\text{tank}} > x_1 > x_2 > x_3 > p_0$,
- $u_4 \neq 0$.

The first condition is fulfilled according to Remark 1, since all parameters a_i are non-zero physical constants. According to Assumption 2, all pressures have non-zero positive values. Therefore, all states are non-zero, fulfilling the second condition. Also the third condition is always fulfilled due to Assumption 1.

Therefore, System (1) is differentially observable (cf. Definition 1) for $u_4 \neq 0$, as all states can be uniquely determined by the outputs and the measurable inputs and their derivatives. As a result, an observer can be implemented to obtain the total pressures and gas partial pressures of the considered fuel cell system with anode recirculation as long as the stack current is not equal to zero (i.e. the fuel cell system is not in idle mode). During the idle mode, all states except for hydrogen partial pressure x_6 can still be determined, since the outputs do not directly depend on it and x_6 is only coupled to the other states via linear multiplication with u_4. Therefore, as long as $u_4 = 0$, the state x_6 has no effect on the other states.

Remark 2: Due to the above discussed coupling between x_6 and u_4, the last state also do not appear in higher derivatives of the outputs as long as $u_4 = 0$. Therefore, the system is not observable of orders $m > 3$ for $u_4 = 0$. □

Since differential observability implies instantaneous observability, not only asymptotic observers, but also finite time observers can be applied to the presented fuel cell system.

Note that from application perspective, instantaneous knowledge about higher derivatives of the inputs and outputs is a strong assumption. However, the required derivations can be specified: according to Equations (10)-(15), $\dot{y}$, $\ddot{y}$, $\dot{u}_1$, $\dot{u}_4$, $\ddot{u}_4$ are required to obtain global differential observability.

Local differential observability

Since global observability has been shown, it is not surprising that also the local condition of differential observability can be shown in the non-idle mode. To do so, it is sufficient to prove that the map $\mathcal{H}_m(x, u^{[m]})$ is injective in a neighborhood $\mathcal{X}_N$ of x^0 [11]. This is usually done by showing that the Jacobian of $\mathcal{H}_m(x, u^{[m]})$ has rank d_x. In the presented case, the Jacobian of the map $\mathcal{H}(x, u^{[3]})$ is a triangular matrix with non-zero elements along the main diagonal. However, it looses its full rank for $u_4 = 0$, since the last entry of the main diagonal is exactly equal to the term $\mathcal{O}_2$ (cf. Appendix). The same holds also for all higher orders $\mathcal{H}(x, u^{[m]})$ due to the already mentioned bilinear term of x_6 and u_4. Thus, local observability also requires $u_4 \neq 0$ and the condition does not hold in idle mode.

However, a similar local observability condition can be obtained, when only the fuel cell voltage y_2 is used as an output and the total pressure y_1 is not measured. To fulfill the rank condition, $\mathcal{H}(x, u^{[m]})$ needs to be at least of dimension d_x. Since System (1) is of dimension $d_x = 6$, and the reduced output function $h_{\text{red}} = x_1$ is of dimension $d_y = 1$, at least five Lie-derivatives are required. Due to the convoluted nature of recurring Lie-derivatives and their resulting Jacobian, those terms were calculated symbolically in MATLAB. Then, the MATLAB toolbox `STRIKE-GOLDD 4.0` [8] was used to prove the rank condition and, consequently, local differential observability.

While this means, that in theory only the measurement of the stack voltage is sufficient to obtain local observability, the numeric evaluation of the involved terms in $\mathcal{H}(x, u^{[6]})$ would be computationally infeasible and, hence, only observers that do not require this map would be applicable in this case.

V. Conclusion and Outlook

In this paper, the observability of total and partial gas pressures in an automotive fuel cell system with anode recirculation is analyzed. In the presented setup, the fuel cell current, the total pressure at the cathode, the opening of the input valve, as well as the opening of the purge valve were assumed as known inputs. By using the fuel cell stack voltage and the total pressure in front of the fuel cell stack as outputs, global differential observability was proven for a stack current not equal to zero. Both sensors are commonly available in automotive fuel cell systems. This global condition was derived by proving that the presented map is globally injective. Since global differential observability implies global instantaneous observability, any asymptotic and finite time observer can be applied to estimate the total pressures as well as the partial gas pressures in front, inside, and behind the fuel cell stack.

A weaker condition could be derived when only the fuel cell stack voltage was used as output. In this case, the fuel cell system is locally differentially observable.

In the future, a finite time observer can be developed to estimate the gas partial pressures in automotive fuel cell systems. A finite time estimation would enable efficient partial gas pressure controls in fuel cell systems, which is crucial for an optimization of hydrogen usage, minimizing the losses during the purge process and reducing the chemical process of degradation. Therefore, the fuel cell system's efficiency and lifetime can be increased.

APPENDIX

Representation of the detailed terms in the calculations of the Lie-derivatives

$$
\begin{aligned}
\mathcal{O}_1(x,u) =& -\left(\frac{a_1}{2\sqrt{x_1-x_2}}+\frac{a_2u_1}{2\sqrt{p_{\text{tank}}-x_1}}\right)\dot{x}_1 \\
&- \frac{a_1(a_{11}u_4 - a_5u_3 - a_4\sqrt{x_1-x_2})}{2\sqrt{x_1-x_2}} \\
\mathcal{O}_2(x,u) =& \frac{a_3a_4a_{13}\sqrt{x_1-x_2}u_4}{x_1x_3x_5} \\
\mathcal{O}_3(x,u) =& -\frac{a_4a_{13}(x_1-2x_2)x_4}{2x_5x_1^2\sqrt{x_1-x_2}}\dot{x}_1 \\
&+\left(\frac{a_6a_{13}(2x_3-x_2)}{2x_2^2\sqrt{x_2-x_3}}-\frac{a_4a_{13}x_4}{2x_1x_5\sqrt{x_1-x_2}}\right)\dot{x}_2 \\
&- \frac{a_6a_{13}}{2x_2\sqrt{x_2-x_3}}\dot{x}_3 \\
&- \frac{a_4a_{13}(x_1-x_2)x_4 - a_{11}a_{13}u_4}{x_1x_5^2\sqrt{x_1-x_2}}\dot{x}_5 \\
&- \frac{a_4a_{13}(x_1-x_2)}{x_1x_5}\left(a_1\frac{x_4}{x_1}+\frac{a_2\sqrt{p_{\text{tank}}-x_1}}{\sqrt{x_1-x_2}}u_1\right) \\
\mathcal{O}_4(x,u^{[3]}) =& -\frac{a_{11}a_{13}}{x_5}\dot{u}_4+\frac{\partial\dot{h}_u(u_4)}{\partial u_4}\frac{\partial u_4}{\partial t}
\end{aligned}
$$

References

[1] J. A. Adams, W. C. Yang, K. A. Oglesby, and K. D. Osborne. The development of Ford's P2000 fuel cell vehicle. *SAE transactions*, pages 1634–1645, 2000.

[2] R. K. Ahluwalia and X. Wang. Buildup of nitrogen in direct hydrogen polymer-electrolyte fuel cell stacks. *Journal of Power Sources*, 171(1):63–71, 2007.

[3] M. Arcak, H. Gorgun, L. M. Pedersen, and S. Varigonda. A nonlinear observer design for fuel cell hydrogen estimation. *IEEE Transactions on control systems technology*, 12(1):101–110, 2004.

[4] K. D. Baik and M. S. Kim. Characterization of nitrogen gas crossover through the membrane in proton-exchange membrane fuel cells. *International Journal of Hydrogen Energy*, 36(1):732–739, 2011.

[5] P. Bernard. *Observer design for nonlinear systems*, volume 479. Springer, 2019.

[6] P Bernard, V Andrieu, and D Astolfi. Observer design for continuous-time dynamical systems. *Annual Reviews in Control*, 53:224–248, 2022.

[7] W. R. W. Daud, R. E. Rosli, E. H. Majlan, S. A. A. Hamid, R. Mohamed, and T. Husaini. Pem fuel cell system control: A review. *Renewable Energy*, 113:620–638, 2017.

[8] S. Díaz-Seoane, X. Rey Barreiro, and A. F. Villaverde. STRIKE-GOLDD 4.0: user-friendly, efficient analysis of structural identifiability and observability. *Bioinformatics*, 39(1):btac748, 2023.

[9] C. Hähnel. *Regelung zum effizienten Betrieb eines PEM-Brennstoffzellensystems*. PhD thesis, Universitätsbibliothek der HSU/UniBwH, 2017.

[10] M. Hauck, F. Petzke, and S. Streif. Model predictive purge control for PEM fuel cell systems with anode recirculation. In *2021 60th IEEE Conference on Decision and Control*, pages 6359–6364. IEEE, 2021.

[11] R Hermann and A Krener. Nonlinear controllability and observability. *IEEE Transactions on automatic control*, 22(5):728–740, 1977.

[12] K. Kodra and Z. Gajic. Order reduction via balancing and suboptimal control of a fuel cell–reformer system. *International journal of hydrogen energy*, 39(5):2215–2223, 2014.

[13] J. M. Lee and B. H. Cho. A dynamic model of a PEM fuel cell system. In *2009 Twenty-Fourth Annual IEEE Applied Power Electronics Conference and Exposition*, pages 720–724. IEEE, 2009.

[14] J. Luna, A. Husar, and M. Serra. Nonlinear distributed parameter observer design for fuel cell systems. *International Journal of Hydrogen Energy*, 40(34):11322–11332, 2015.

[15] J. Luna, E. Usai, A. Husar, and M. Serra. Nonlinear observation in fuel cell systems: A comparison between disturbance estimation and high-order sliding-mode techniques. *International Journal of Hydrogen Energy*, 41(43):19737–19748, 2016.

[16] B. A. McCain, A. G. Stefanopoulou, and J. B. Siegel. Controllability and observability analysis of the liquid water distribution inside the gas diffusion layer of a unit fuel cell model. 2010.

[17] J. Morales, C. Astorga, J. Reyes, U. Cano, and P. Cruz. Application of a nonlinear observer for estimation of variables in a PEM fuel cell system. *Journal of the Brazilian Society of Mechanical Sciences and Engineering*, 39:1323–1332, 2017.

[18] M. Obermaier, M. Rauber, A. Bauer, T. Lochner, F. Du, and C. Scheu. Local fuel starvation degradation of an automotive PEMFC full size stack. *Fuel Cells*, 20(4):394–402, 2020.

[19] J. T. Pukrushpan, H. Peng, and A. G. Stefanopoulou. Control-oriented modeling and analysis for automotive fuel cell systems. *J. Dyn. Sys., Meas., Control*, 126(1):14–25, 2004.

[20] A. Rabbani and M. Rokni. Effect of nitrogen crossover on purging strategy in PEM fuel cell systems. *Applied energy*, 111:1061–1070, 2013.

[21] P. Swain and D. Jena. PID control design for the pressure regulation of PEM fuel cell. In *2015 International Conference on Recent Developments in Control, Automation and Power Engineering (RDCAPE)*, pages 286–291. IEEE, 2015.

[22] R. Vepa. Adaptive state estimation of a PEM fuel cell. *IEEE Transactions on Energy Conversion*, 27(2):457–467, 2012.

[23] B. Wang, H. Deng, and K. Jiao. Purge strategy optimization of proton exchange membrane fuel cell with anode recirculation. *Applied energy*, 225:1–13, 2018.